Published in final edited form as:
Neuroimage. 2010 January 15; 49(2): 1559–1571. doi:10.1016/j.neuroimage.2009.08.064.

FLAIR SIGNAL AND TEXTURE ANALYSIS FOR LATERALIZING MESIAL TEMPORAL LOBE EPILEPSY

Kourosh Jafari-Khouzani[a], **Kost Elisevich**[b], **Suresh Patel**[a], **Brien Smith**[c], and **Hamid Soltanian-Zadeh**[a,d]

[a]Department of Diagnostic Radiology, Henry Ford Hospital, Detroit, MI 48202, USA

[b]Department of Neurosurgery, Henry Ford Hospital, Detroit, MI 48202, USA

[c]Department of Neurology, Henry Ford Hospital, Detroit, MI 48202, USA

[d]Control and Intelligent Processing Center of Excellence, Electrical and Computer Engineering Department, University of Tehran, Tehran 14395-515, Iran

Summary

Standard magnetic resonance (MR) imaging analysis in several cases of mesial temporal lobe epilepsy (mTLE) either fail to show an identifiable hippocampal asymmetry or provide only subtle distinguishing features that remain inconclusive. A retrospective analysis of hippocampal fluid-attenuated inversion recovery (FLAIR) MR images was performed in cases of mTLE addressing, particularly, the mean and standard deviation of the signal and its texture. Preoperative T1-weighted and FLAIR MR images of 25 nonepileptic control subjects and 36 mTLE patients with Engel class Ia outcomes were analyzed. Patients requiring extraoperative electrocorticography (ECoG) with intracranial electrodes and thus judged to be more challenging were studied as a separate cohort. Hippocampi were manually segmented on T1-weighted images and their outlines transposed onto FLAIR studies using an affine registration. Image intensity features including mean and standard deviation and wavelet-based texture features were determined for the hippocampal body. The right/left ratios of these features were used with a linear classifier to establish laterality. Whole hippocampal within-subject volume ratios were assessed for comparison. Mean and standard deviation of FLAIR signal intensities lateralized the site of epileptogenicity in 98% of all cases, whereas analysis of wavelet texture features and hippocampal volumetry each yielded correct lateralization in 94% and 83% of cases, respectively. Of patients requiring more intensive study with extraoperative ECoG, 17/18 were lateralized effectively by the combination of mean and standard deviation ratios despite a ratio of mean signal intensity near one in some. The analysis of mean and standard deviation of FLAIR signal intensities provides a highly sensitive method for lateralizing the epileptic focus in mTLE over that of volumetry or texture analysis of the hippocampal body.

Keywords

Temporal lobe epilepsy; FLAIR signal; Texture analysis; Volumetry

Introduction

Mesial temporal lobe epilepsy (mTLE) is the most commonly investigated and operated form of localization-related epilepsy. Clinical study of this disorder has become increasingly more

Corresponding Author: Kourosh Jafari-Khouzani, Dept. of Diagnostic Radiology, Henry Ford Hospital, One Ford Place, 2F, Detroit, MI 48202, USA, Phone: +1-313-874-4378, Fax: +1-313-874-4494, kjafari@rad.hfh.edu.

elaborate, particularly through electrographic and imaging applications, with the intent of arriving at a means of establishing the laterality of the epileptic focus with as much certainty as possible. Such certainty is critical in order that surgical outcomes are optimized (Engel, 1987). Hippocampal neuronal loss and gliosis of variable degree and distribution within its subfields dominate the pathology in resected material although several specimens show only subtle change or no abnormality. Likewise, magnetic resonance (MR) imaging in mTLE identifies a wide range of features, the most characteristic of which has been mesial temporal sclerosis (MTS) that is defined, in part, as a volume reduction of the hippocampus in T1-weighted images (Cendes et al., 1993; Jack et al., 1990; Kim et al., 1994) and an increase in signal intensity in both T2-weighted and fluid-attenuated inversion recovery (FLAIR) images (Jack et al., 1994; Jack et al., 1996). Such features often declare a site of epileptogenicity, although, in 15 – 30% of mTLE cases no clear asymmetry in volume between the hippocampi is noted despite clear indication of ictal origin in the area (Carne et al., 2004; Jackson et al., 1994; Van Paesschen, 1997). Qualitative assessments lack sufficient rigor to declare laterality in some mTLE cases in which the difference in signal intensities is minor (Van Paesschen, 1997).

Image analysis of cerebral tissue involves an evaluation of structural features and signal intensity. It implements statistical measures to assess the size, shape, signal and texture of a particular region of interest. Fluid-attenuated inversion recovery MR imaging provides a measure of free water and the extent of gliosis in a given location and has become standard in the investigation of localization-related epilepsy; yet, as in the case of volumetric analysis, clinical experience has shown that its application has lacked sufficient sensitivity in some cases of mTLE, particularly those lacking MTS, as will be shown in the current paper. Texture analysis has been used in the analysis of several clinical conditions, notably Alzheimer's disease (Freeborough and Fox, 1998; Kodama and Takeuchi, 2005), multiple sclerosis (Yu et al., 1999), cerebral neoplasia (Herlidou-Meme et al., 2003), and schizophrenia (Liu et al., 2004). The analysis provides information regarding the periodicity of signal intensity patterns generated in MR images of tissues. Alterations in these signal patterns appear to correlate with histopathological changes in the region of interest. Using combined texture and discriminant analyses based on pixel pattern anomalies in MR images, Yu *et al.* (Yu et al., 2002) detected changes in the cerebral cortex in the lithium-pilocarpine rat model of chronic epilepsy at sites associated with focal epileptogenicity in 16 animals, 10 of which showed no focal changes, otherwise, on T2-weighted images. The application of texture analysis to human epilepsy, particularly mTLE, has shown similar promise. Hippocampal sclerosis can be distinguished from the normal state (Bonilha et al., 2003). Moreover, the contralateral hippocampus is found to harbor abnormal textural features in cases otherwise too subtle to detect any appreciable changes using other MR imaging applications (Yu et al., 2001). Its use has also been extended to the detection of focal cortical dysplasia, a common and elusive substrate of focal epileptogenicity (Antel et al., 2003; Bernasconi et al., 2001).

In order to establish the relative efficacy of measuring the mean and standard deviation of FLAIR signal intensity values and of textural analysis, a retrospective comparative assessment was undertaken in cases of unilateral mTLE. Only those rendered without seizures postoperatively were chosen for study in order to establish a genuine criterion for laterality. In particular, attention was drawn to a subset of this cohort that required extraoperative electrocorticography (ECoG) with intracranially implanted electrode arrays as such cases are considered more challenging due either to a lack of any asymmetry of imaging features or electrographic discordance with imaging findings. In the former situation, disparity in volume may not be accompanied by a clear asymmetry in FLAIR signal intensity or, conversely, a subtle asymmetry in signal intensity may be found in volumetrically similar hippocampi of normal or reduced size.

T2 relaxometry of the hippocampus has been promoted for use in lateralizing the epileptic focus in mTLE (Bernasconi et al., 2000; Briellmann et al., 2002; Coan et al., 2006; Grunewald et al., 1994; Jack, 1996; Jackson et al., 1993; Okujava et al., 2002; Woermann et al., 1998). Specifically, a prolonged T2 relaxation time has been associated with hippocampal sclerosis. The hippocampus has also been studied in sequential coronal profile to establish whe ther local alterations are more prevalent within the structure in cases of mesial temporal epilepsy (Woermann et al., 1998). Measurable variation in T2 relaxation times was identified along the anteroposterior axis although a quantitative analysis was not performed. We have chosen to evaluate FLAIR signal intensity. It has been shown that use of cerebrospinal fluid (CSF)-nulling in FLAIR MR imaging has helped to improve the precision of hippocampal T2 measurements (Melhem et al., 1998). Indeed, increased T2 values in the hippocampus could ostensibly be affected by CSF in the neighboring frequently enlarged temporal horn, rather than by overt tissue changes in the hippocampus (Shorvon, 1994). We have chosen also to study the pattern of FLAIR signal intensity variations throughout the hippocampus to establish whether the extent of variation may be an additional reliable factor in lateralizing the epileptic focus.

Materials and Methods

Patients

An archival review of patients operated for mTLE by a single surgeon (KE) during a nine year period (1998 – 2007) yielded 36 patients (11 males, 25 females) with a mean age of 39 years (range 14 – 66 years) (Table 1). Only those patients rendered free of seizures postoperatively (Engel class Ia), as defined by the Engel classification for surgical outcome, were included in the analysis (Engel, 1987). The patients had sufficient clinical followup (7.6±4.4, 2–11 years). All patients underwent video-electroencephalographic (EEG) inpatient assessment over a minimum three day period, MR imaging, sodium amobarbital study and neuropsychological assessment. Patients with major motion artifact in their MRI (13% of the archived population) were excluded. Eighteen (4 males, 14 females) of the 36 patients (50%) required extraoperative ECoG with intracranially implanted electrode arrays. Several different neuroradiologists rendered impressions of the appearance of the mesial temporal structure in each patient at the time of the initial report. The text of these original reports was reviewed by the authors and all MR images reexamined to render a final impression of MTS according to the following criteria: 1. Reduction of hippocampal volume as determined by a right-left asymmetry on T1-weighted coronal images, 2. Increased FLAIR MR signal intensity and, 3. Loss of intrinsic hippocampal laminar structure. These features were required on at least two sequential coronal images to declare the impression of MTS. A single feature such as volume loss alone would therefore not support this impression. Ictal and interictal single photon emission computed tomography (SPECT) was performed in most of the patients and magnetoencephalography (MEG) in select patients. Those in whom ambiguity regarding laterality of the focus remained, intracranial electrodes were implanted for extraoperative ECoG.

Control subjects were neurologically intact, nonepileptic individuals without overt lesional pathology on imaging. A total of 25 subjects were drawn from an archive of control subjects in a sleep research project.

MR Imaging

Magnetic resonance imaging was acquired with a General Electric 1.5-T Signa system (GE Medical Systems, Milwaukee WI). All subjects underwent coronal T1-weighted MR study using a spoiled gradient-echo (SPGR) sequence with TR/TI/TE = 7.6/1.7/500 ms, flip angle = 20°, field of view (FOV) = 200×200 mm^2, matrix size = 256×256, pixel size = 0.781×0.781 mm^2, slice thickness = 2.0 mm (voxel size =0.781×0.781×2.0 mm^3), number of slices = 124,

bandwidth 25 kHz, and scanning time of 5 minutes and 45 seconds. Coronal FLAIR MR data sets were acquired with TR/TI/TE = 10002/2200/119 ms, flip angle = 90°, FOV = 200×200 mm^2, matrix size = 256×256, pixel size = 0.781×0.781 mm^2, slice thickness = 3.0 mm (voxel size =0.781×0.781×3.0 mm^3), minimum number of slices = 47, bandwidth 20.8 kHz, and scanning time of 12 minutes. When required, translational corrections were made to correct for head position from slice-to-slice. Most adjustments were made in the dorsoventral direction.

The regions of interest (ROIs) encompassing the hippocampi were outlined manually for segmentation using sequential coronal T1-weighted MR images (Fig. 1) with reference to an MRI atlas identifying the hippocampus (Duvernoy, 2005). A single investigator (KJ) outlined all coronal hippocampal contours (usually 20 slices/case) using Eigentool an in-house software (http://www.radiologyresearch.org/eigentool.htm). These were then verified by two other investigators (KE and SP). The accuracy of current automatic hippocampal segmentation techniques was judged insufficient to reliably avoid contamination of the FLAIR signal intensity measure with unwanted signal from outside the intended ROI, although they may have acceptable performance for hippocampal volumetry (Chupin et al., 2009;Hammers et al., 2007;Rodionov et al., 2009). Manual segmentation was used to minimize such an error. The method of Kim et al (1994) was used to establish anterior and posterior boundaries for hippocampal FLAIR analysis (Kim et al., 1994). This approach reduced the impact of the partial volume effect upon such analysis. The anterior coronal boundary plane coincided with the gyrus intralimbicus, whereas the posterior plane was that of the most caudal section through the quadrigeminal plate. For volumetric analysis, the entire hippocampus was examined. The volumes in each case were calculated by summing the area of the ROIs outlining the hippocampus on successive sections and multiplying by the section thickness. Only the brain was segmented by withdrawal of all other tissues using Brain Extraction Tool (BET) (Smith, 2002). This step improves the accuracy of subsequent coregistration which, as will be explained, is important in quantitative measurements. The T1-weighted and FLAIR MR image sets were coregistered using a rigid registration technique (FLIRT) (Jenkinson and Smith, 2001) based on mutual information and the manually segmented ROIs were mapped onto the FLAIR MR image set using the registration parameters. These were then used for feature extraction. Imprecise hippocampal segmentation and coregistration could result in misallocation of ROIs on corresponding FLAIR images with the inclusion of unwanted sites containing disparate signal intensities (i.e., cerebrospinal fluid) which could markedly affect the range and mean estimates. To this end, the segmentation and coregistration outcomes were cross-checked using Eigentool. Specifically, new ROIs were placed on brain landmarks of the coregistered T1-weighted images. These were then loaded into the FLAIR image dataset and rechecked for correct placement. No misalignment was found between coregistered T1-weighted and FLAIR images.

Feature Extraction

Three sets of features were extracted from each hippocampal ROI: mean and standard deviation of the FLAIR MR signal intensity, wavelet transform-derived energy and volumetry. The final value for each feature was expressed as a ratio of measured values of the two hippocampi for normalization purposes and to facilitate the classification and graphical analysis of left- and right-sided epileptogenicity. A ratio of FLAIR signal intensity features was used to avoid the problem of variance in FLAIR signal intensity from case-to-case and scan-to-scan. Establishing an internal reference is not a trivial undertaking although a ratio is generally less affected by imaging imperfections. Hippocampal volumes were normalized to the intracranial volume as measured using BET.

(i) Mean and Standard Deviation—Hippocampal FLAIR signal intensity is increased in association with a focal epileptogenicity as a consequence of gliosis and increased water

content in the region. In the presence of an increased mean signal intensity, there is greater slice-to-slice variability attributable to nonuniformity in the extent of gliosis throughout the hippocampus (Fig. 2). The combination of these two values was used as an added measure of hippocampal asymmetry.

(ii) Wavelet Transform—Wavelet transform analysis provides a frequency content of an image by representing a signal as a linear combination of basis functions such as Daubechies wavelet bases (Daubechies, 1992) which are scaled and translated copies of the waveform. Coefficients of the basis functions correspond to different scales and frequency directions of the signal. For each pixel of an image, the wavelet coefficients characterize the point-specific frequency content of the image over a set of scales. By a serial application of filters, wavelet decomposition results in the production of subbands each of which is represented by a set of coefficients of basis functions in a single frequency domain (Mallat, 1999). For images, each level of ordinary wavelet decomposition produces three subbands (Fig. 3). The ordinary wavelet transform is, however, not translation-invariant. Translation-invariant wavelet decomposition was used in this analysis to produce more reliable features (Pesquet et al., 1996). The size of the produced subbands for translation-invariant decomposition is equal to the image size. An energy feature representing the strength of the coefficients in a subband may be calculated for each subband and used to evaluate texture properties of an image.

For each hippocampal ROI, two levels of translation-invariant wavelet transform were calculated to produce seven subbands, similar to ordinary wavelet transform depicted in Fig. 3. The energy (E_k) feature was calculated as follows for each subband:

$$E_k = \frac{1}{MN} \sum_{i=1}^{M} \sum_{j=1}^{N} I_k^2(i, j) \tag{1}$$

where $I_k(i,j)$, $k = 1,2,\ldots,7$ is the kth subband with dimensions $M \times N$. All ROIs with sizes less than 8×8 pixels were eliminated. Since the segmented hippocampal ROIs are not rectangular, the sharp edges resulting from zero intensities outside the hippocampus (Fig. 4) significantly affect the wavelet coefficients (Garcia-Sevilla and Petrou, 2001). To reduce this effect, rectangular ROIs were generated by filling out the empty areas using a texture inpainting technique based upon exemplar-based texture synthesis (Criminisi et al., 2004;Efros and Leung, 1999), which is illustrated in Fig. 4. Each ROI is first inscribed in a rectangle, then dilated repeatedly using a 3×3 window (Jafari-Khouzani et al., 2003). The dilated part is filled pixel-by-pixel by finding similar neighborhoods within the image. The image is repeatedly propagated through its boundary until the empty area is filled. In this way, seven energy features are created for each ROI. The features are then averaged over the hippocampal ROIs in different slices to create 7 energy features for each hippocampus.

Three-dimensional texture analysis could outperform the 2D analysis described above, although, the large slice thicknesses (3mm) of FLAIR images compared to the pixel size (0.781 mm) and the large empty area of the rectangular prism inscribing the whole hippocampus might limit the reliability of such 3D analysis.

Even length filters have been suggested for wavelet texture analysis (Mojsilovic et al., 2000). Daubechies wavelet bases with even wavelet lengths, 2, 4,…, 20, were analyzed without observing significant differences in lateralization. The results of using Daubechies wavelet bases with wavelet lengths, 4, 6 and 8, are reported. We also tested Coiflets and biorthogonal wavelet bases (Daubechies, 1992) without observing a significant difference either.

(iii) Volume—Hippocampal volume reduction correlates favorably with the side of mTLE (Cendes et al., 1993). The volumes of both left and right hippocampi were established from manually drawn ROIs and then normalized to (i.e., divided by) the intracranial volume using BET.

Classification

Each case of mTLE was classified into left-sided or right-sided epileptogenicity using a linear discriminant function, $f(X) = W \cdot X + B$, where $X = [x_1,\ldots,x_n]^T$ is the vector of features calculated for each patient (i.e., the ratios of left and right hippocampal features), n is the number of features, and $W = [w_1,\ldots,w_n]$ and B are the classifier parameters. A discriminator line is provided graphically by using some simple training techniques such as the Fisher linear discriminant analysis (Theodoridis and Koutroumbas, 2006). The latter technique maximizes the ratio of 'between class distance' and 'within class distance' for any given set of features. For intensity-based features (mean, standard deviation, and texture features), a boundary domain on either side of the discriminator line was established by introducing parallel boundary lines at 0.25 standard deviation (SD) separation from the discriminator line. This provides some estimation of the number of cases in which the chosen feature analysis indicates a relatively fine separation of laterality.

To test the linear separability of the samples, we trained the classifier using all data samples and reported the resulting classification accuracy. Accuracy is defined as the ratio of the number of misclassified patients to the total number of patients based on the defined boundaries for each class. As might be expected, control subjects tended to cluster within the feature space along the discriminator line, as will be presented later. The laterality of the mTLE in certain study patients may be separable by the discriminator line but yet may appear within the boundary domain.

The volume feature set analysis was expressed in linear fashion with a clustering of volume ratios of control subjects around the unity line. Boundary margins were defined here by the extremes of the distribution of this control cluster set.

Results

Patients

In the entire group, the epileptic focus resided on the right in 16 cases (44%) and on the left in 20. The mean duration of epilepsy was 27 years (range 4 – 50 years). Risk factors were established in all but six patients with the proviso that the strength of the causation may be variable from case-to-case. Early childhood febrile seizures were definitively reported in seven cases, moderate to severe closed head injury with a loss of consciousness exceeding 30 minutes in duration (Annegers et al., 1998) in 11 cases with a single case of overlap of the two factors. An infectious etiology was raised in five cases and a family history of epilepsy was noted in eight cases. Hippocampal pathology was not available in seven cases although in three cases, gliosis was identified in the temporopolar tissue. There appeared to be no distinctive clinicopathological correlation between risk factor and histopathology. The largest etiological grouping, that of closed head injury, was found to manifest an Ammon's horn sclerosis in only 45% of cases. Hippocampal sclerosis of varying severity and characterized by pyramidal and/or dentate granule cell dropout, gliosis and, in most cases, corpora amylacea was found in 21 cases. Among these cases, preoperative imaging reports of mesial temporal sclerosis (MTS) were found in 17 (81%). Of the 18 cases requiring extraoperative ECoG, 9 (50%) harbored a histologically sclerotic hippocampus and preoperative imaging declared an MTS in 10 cases (55%). Only 6 cases showed overlap of these attributes, although, in one other case of MTS, the hippocampal histology was unavailable.

The control group contained 25 subjects (13 males, 12 females) with a mean age of 32 y (range 19 – 53 y). Although the range and mean value of ages in this group is different from the patient group, further analysis, in fact, shows insufficient correlation between the extracted features and age. For example, the correlations between age and FLAIR mean signal intensity, FLAIR standard deviation and volume ratios were −0.31 (p=0.06), −0.22 (p=0.19), 0.27 (p=0.11), respectively, for the patient group and 0.03 (p=0.89), −0.12 (p=0.57), −0.34 (p=0.09) for the control group.

Comparative Feature Set Analysis

Each feature set was examined separately using a linear discriminant function. Table 2 summarizes the results of applying each of these sets to the study population as a whole with the boundary domain both included and excluded. Of the sets examined, the combined features of the mean and standard deviation of FLAIR signal intensity proved to be the most closely in agreement with the presence of left- or right-sided epileptogenicity. This feature set combination yielded an accuracy of 98% compared with those of the individual sets that yielded a 98% accuracy for the standard deviation measure of FLAIR signal intensity and only a 86% accuracy for the mean FLAIR signal intensity. When the boundary domain was taken into account, accuracies of 72% for standard deviation, 58% for mean and 75% for their combination were obtained.

A scatter plot of mean and standard deviation features shows the expected cluster of control subjects at unity (Fig. 5). Despite this, there were four outliers, still contained in the boundary domain in the graphic analysis of FLAIR mean signal and standard deviation. These outliers retained volume symmetry. Of the four, two were in the immediate vicinity of the central cluster, whereas the remaining two harbored a mean signal intensity that was preferentially left in one case and right in the other. These cases were admixed among the epilepsy cases that required extraoperative ECoG (Fig. 5B) underlining the difficulty, at times, in distinguishing some of the epilepsy cases from the nonepileptic condition. The mean ratio is different among groups of patients with left-sided and right-sided mTLE and control subjects ($p<4.0\times10^{-6}$) with a 95% confidence interval of [−0.0422 – 0.0149] between left-sided mTLE patients and control subjects, [0.0365 – 0.0657] between right-sided mTLE patients and control subjects and [−0.0788 – −0.0483] between left-sided and right-sided mTLE patients. The standard deviation ratio is different among these same groups ($p<10^{-12}$) with a 95% confidence interval of [−0.25 – −0.17] between left-sided mTLE patients and control subjects, [0.18 – 0.26] between right-sided mTLE patients and control subjects and [−0.43 – −0.35] between left-sided and right-sided mTLE patients. A linear discriminator shows a distinctive separation of cases representative of left- and right-sided epileptogenicity. A boundary margin of +/− 0.25 SD was created to establish the distribution of cases judged to be marginal from those more definitive by the measure applied. Patients showing the greatest asymmetry in signal intensity features of the hippocampi on FLAIR MRI (Fig. 6) were located further from the discriminator line.

Those patients requiring extraoperative ECoG in order to definitively lateralize the site of temporal lobe epileptogenicity were segregated as a separate cohort in order to establish whether the same analysis might specifically address a population in which conventional noninvasive investigation has failed to establish laterality. Of these 18 cases, 13 were judged to have overt features of MTS or a distinct volumetric asymmetry (volumetric difference > 500 mm^3) (Table 1). Twenty-two percent (4/18; cases 1, 11, 13, 15) of such patients were found to have qualitatively similar hippocampi on the right and left (Table 1). In fact, where no asymmetry could be discerned whatsoever by visual inspection (Fig. 7, Fig. 8), the FLAIR features of mean signal intensity and standard deviation in the majority of patients approached the discriminator line, falling within the boundary margins. Of the 18 patients undergoing

invasive study, 9 (50%) were found outside the boundary margins whereas the remainder were found within.

Texture Analysis

The Daubechies wavelet bases with lengths db4, db6 and db8 were used to calculate the wavelet features as previously described. Seven features for each of these wavelet bases were extracted. By testing all two-dimensional feature spaces, two features were identified that separated left- from right-sided epileptogenicity with maximal accuracy (Table 2). A maximum correct outcome classification percentage of 94% was obtained using the two wavelet energy features (E_1 and E_2) with wavelet basis db8, in particular (Fig. 9). A scatter plot of the two selected wavelet energy features shows a separation of left- and right-sided epileptogenicity by a linear discriminator with a central clustering of nonepileptic control subjects.

As in the previous analysis with the FLAIR mean signal and standard deviation measure (Fig. 5B), a similar study of the cohort of patients requiring extraoperative ECoG was performed to establish whether texture analysis might provide comparatively equivalent or complementary information regarding the separation of laterality of focal epileptogenicity (Fig. 9B). The majority of controls (84%) fall within the boundary domain. There were ten patients who were found within the boundary domain and had required extraoperative ECoG, indicating only subtle textural distinctions between such cases and those which were not epileptic. Only two patients (11%), from those who did not require further invasive study, approached the discriminator line. Eleven patients located within the boundary domain were still correctly lateralized according to the side of their focal epileptogenicity.

Volume Analysis

Hippocampal volumes were calculated for all patients and controls and normalized to the intracranial volume (Fig. 10). Accuracy by outcome classification using this measure (i.e., the right/left hippocampal volume ratio, also specified in Fig. 10 by the $y=x$ discriminator line) was found to be 83%. A separation of patients requiring extraoperative ECoG identified five patients falling between boundary margins defined as containing the cluster of control subjects. Four patients with a right-sided mTLE were found to have hippocampi of a relatively larger volume in comparison to the left side and all required invasive monitoring to distinguish their laterality. Three other patients with a right-sided mTLE still required invasive study despite harboring a smaller hippocampal volume on the right as a result of other ambiguities arising in their preliminary investigation. Of those with a left-sided mTLE, no patient who proceeded to surgery without extraoperative electrocorticography was found within the boundary margins. However, three other left-sided mTLE patients required invasive study because of other ambiguities noted in their investigations.

Misclassified and Boundary Domain Cases

Although each of the three feature sets studied, FLAIR signal intensity and standard deviation, wavelet analysis and volumetry, demonstrated flaws in their respective applications, all showed potential benefit in lateralizing mTLE by using combinations of them. The criterion for inclusion in the boundary domain required the Euclidean distance from the discriminator line to be less than 0.25 of the average standard deviation of the samples in each of the two feature sets of FLAIR signal intensity and standard deviation and wavelet analysis. The boundary domain in the case of volume analysis was simply defined by the linear distribution of volumes of control subjects clustered around $y=x$ line. Table 3 details all cases of mTLE that were misclassified according to the discriminator line or allocated in the boundary domain according to each of the three measures used in the present study. Use of the FLAIR mean signal and standard deviation yielded only a single misclassification (case 9) and eight other cases situated in the boundary domain, equally distributed as left- or right-sided mTLE on either side of the

discriminator line. Boundary domain samples identified in one feature space could also be found to be misclassified in another feature space as with case 8 found within the boundary domain of the FLAIR mean and standard deviation measure but misclassified by the wavelet signature measure. One (case 9) remained misclassified by two measures and was within the boundary domain of the third measure. This finding diminishes the chance of achieving absolute reliability by combining features despite the fact that a number of misclassified cases (5, 8, 11, 15, 16, 18, 29) in one feature space could be correctly classified in other feature spaces.

Ammon's Horn Sclerosis

Twenty-one of the 36 cases of mTLE were found to have AHS. These cases were isolated as a separate cohort to establish whether this histopathological entity might be better lateralized by the application of FLAIR MR mean signal intensity and standard deviation. Careful analysis (Fig. 5E) shows that there is no clear separation of cases with and without AHS although there is a greater central clustering of those cases without AHS around unity using the mean ratio measure. There is also a tendency to cluster cases of AHS in the expected extreme distributions for respective left- and right-sided epileptogenicity. The latter again indicates the tendency for higher and more variable FLAIR MR signal intensities in cases of AHS.

Discussion

The combined application of the FLAIR mean signal intensity measure and its standard deviation in the hippocampus provides an effective means of distinguishing the laterality of mTLE. An accurate estimation was achieved in 98% of cases, leaving only a single case misclassified. The same case with several others was misclassified by volumetry. Perhaps, more importantly, those cases that required extraoperative ECoG and, therefore, were judged to have sufficient ambiguity in lateralization by conventional noninvasive study, could be distinguished by the application of FLAIR mean signal intensity and its standard deviation. This provides ample evidence of the utility of signal intensity measures in determining the site of ictal origin and underlines the importance of the study of intrinsic changes in the hippocampal structure as a consequence of the cause or the process of epileptogenesis.

Linear classifiers were applied in order to establish laterality by the creation of a discriminator line separating right- from left-sided mTLE. A boundary domain was then created to ascertain the number of cases approaching the discriminator line for each measure. Of the three measures analyzed, the greatest number of cases contained within the boundary domain or immediately adjacent to it belonged to that of the FLAIR wavelet features suggesting that the qualitative separation of right- from left-sided epileptogenicity on the basis of FLAIR texture analysis would have been difficult in several individuals. Despite their proximity to the discriminator line, all but one (case 9) of these cases were correctly allocated as right- or left-sided mTLE by mean signal intensity and standard deviation. This was a 40 year old female with a 19 year history of posttraumatic mTLE in whom routine imaging had demonstrated an apparent reduction in hippocampal volume on the left without asymmetry in signal intensity. Ictal and interictal SPECT did not reveal an epileptogenic focus. Video-scalp electroencephalographic study of this patient was insufficiently lateralizing requiring intracranial electrode placement targeting both mesial temporal lobe structures, in particular. This finally declared a unilateral epileptogenicity allowing a right-sided mesial temporal lobe resection. Image analysis with FLAIR mean signal intensity and standard deviation erroneously identified the left side as epileptogenic. A hippocampal malrotation on the left (Fig. 11) may underlie a developmental anomaly that resulted in this epileptogenicity (Fernandez et al., 1998;Lehericy et al., 1995). The great majority of misclassified cases, otherwise, could be found within the linear boundary domain of each feature set. In the wavelet feature set in Fig. 9, case 29 was not found within

the linear boundary domain. In the volume feature set were certain misclassified cases (5, 9, 18) not found within the linear boundary domain. Otherwise, a variety of cases misclassified using one measure could be found correctly lateralized in the boundary domain of another measure.

For the patient group, the hippocampal volume ratio (right/left) had correlations of −0.51 ($p<0.0014$) and −0.76 ($p<9.0\times10^{-8}$) with FLAIR mean and standard deviation signal intensity features, respectively. In a previous study (Van Paesschen et al., 1995), the ratio of hippocampal T2 measurements (right/left) had a correlation of −0.91 ($p<0.0001$) with the volume ratio (right/left). Differences in the respective patient populations and imaging measures will likely account for the difference in correlation seen between these two studies. Moreover, the current results underline the usefulness of FLAIR MR imaging as an independent attribute.

In some coronal images, spurious dark spots have been noted to appear in the hippocampal formation on T1-weighted and FLAIR MRI studies; these may represent dilated Virchow-Robin spaces (Heier et al., 1989; Maclullich et al., 2004). Otherwise, they could represent unobliterated parts of the hippocampal sulcus (Duvernoy, 2005). Their presence results in a reduction of the hippocampal mean signal intensity to a variable degree but, more importantly, may result in a greater variance of signal and, therefore, influence the linear separability of the samples by the standard deviation measure. It is difficult to declare whether this might have been the case in the single misclassified example.

Increased signal intensity in the hippocampal formation in cases of mTLE has been demonstrated by a number of MR image contrast applications. Prior to the introduction of FLAIR MR imaging, conventional T2-weighted images correctly lateralized the site of epileptogenicity in 91% of cases, whereas T2-weighted fast spin echo (SE) and proton density-weighted images were accurate in 84% and 72% of cases, respectively (Jack et al., 1994). When double SE and FLAIR pulse sequences were applied in a separate comparative study of 36 patients using an identical standardized imaging protocol, an accuracy of 91% and 97%, respectively, was achieved (Jack et al., 1996). In the latter study, 32 patients (89%) were shown to have histopathological evidence of AHS and no comparative hippocampal volumetry was performed. Moreover, a postoperative assessment of epilepsy status was not provided to establish unequivocally, whether the medial temporal structure was ultimately the site of epileptogenicity. In the current study, 21/36 patients (58%) were shown to have AHS although five others were not studied histologically. Two of the five cases were judged not to show MTS as reported qualitatively although volumetric differences ($> 500\ mm^3$) were identified for both (cases 3, 18). Including these five cases in the AHS-positive group would increase the population to 72% (26/36). Thus, despite the uniformity of postoperative outcome (i.e., Engel class Ia), a greater variation of presentation was identified at outset in comparison to that of the previous study (Jack et al., 1996).

Other MR applications have been used to address the lateralization problem in mTLE. The apparent diffusion coefficient (ADC) has been found to be significantly reduced in the putatively epileptogenic medial temporal lobe (O'Brien et al., 2007; Wehner et al., 2007). However, in a subgroup of patients with mTLE who had nonlateralizing conventional MR imaging studies, no significant difference in the ADC from the contralateral side was identified (Wehner et al., 2007). Contrast-enhanced MR perfusion-weighted image analysis has shown a reduced cerebral blood flow ratio ipsilateral to the side of ictal electroencephalographic onset including two cases in which conventional MR imaging failed to distinguish the putative epileptogenic site (O'Brien et al., 2007). Further study was considered necessary to confirm preliminary findings. The use of functional imaging has provided further lateralizing capability. Subtraction ictal SPECT coregistered to MRI (SISCOM) has changed the course of investigation sometimes obviating the need for intracranial electrode implantation (Tan et al.,

2008). Fluorodeoxyglucose-positron emission tomography (FDG-PET) is useful for TLE lateralization (Gambhir et al., 2001) and routinely used by many centers. PET of serotonin (HT_{1A}) receptor binding has identified reduced uptake in temporal lobe epileptic foci (Didelot et al., 2008; Toczek et al., 2003) even in the absence of pathological changes or neuronal loss (Merlet et al., 2004).

Hippocampal volumetry and FLAIR signal intensity have been helpful as qualitative measures in defining mesial temporal sclerosis. Several cases are marked by subtle differences of either feature and this lack of clear distinction often creates sufficient ambiguity to warrant further intensive study with extraoperative ECoG. Application of quantitative hippocampal volumetry alone, in the present study of 36 definitive cases of mTLE identified a correct lateralization in 83%, in keeping with published results (Jackson et al., 1994). The mean signal intensity of hippocampal FLAIR MR image data, on the other hand, proved to be somewhat more lateralizing with 86% of cases correctly identified. This study supports the notion that MR image postprocessing analysis has more to add to improve upon the means by which the laterality of mTLE may be established. The combined use of T2 relaxometry and volumetry in the case of mTLE was shown to be a reliable method for identifying hippocampal sclerosis in approximately 80% of cases (Van Paesschen, 1997). Experience with familial mTLE, however, has established that a significant proportion (34%) of asymptomatic first degree relatives of afflicted patients were found to have features of MTS, including both hippocampal atrophy and T2 signal hyperintensity (Kobayashi et al., 2003). Such findings should temper enthusiasm towards drawing too strong a conclusion regarding focal epileptogenicity. Greater attention to FLAIR signal analysis, specifically the mean signal intensity and the variation of signal along the hippocampal axis may add further to the reliability of imaging methods in identifying the site of ictal onset in mTLE.

The histopathological change underlying a focal epileptogenicity is ostensibly a nonuniform process and, in the context of a uniformly structured entity such as the hippocampus, it may therefore give rise to some variation along its longitudinal axis as suggested by prior study (Babb and Jann Brown, 1987; Woermann et al., 1998). Sporadic and subsegmental cell loss with accompanying deposition of corpora amylacea and varying degrees of gliosis underlie this variation. This, in turn, is expressed by alterations in FLAIR MR signal intensities in sequential coronal images along the anteroposterior axis of the hippocampus. Both the standard deviation of the mean signal intensity and wavelet texture signatures are, accordingly, affected by such change. The relative strength of these measures was, therefore, assessed in order to determine whether their applications could be complementary. Texture analyses currently are based on side-to-side comparisons and therefore may be insensitive in cases of bilateral disease or in familial TLE cases (Kobayashi et al., 2003).

Texture analysis by wavelet transform independently lateralized cases of mTLE correctly in 94% of cases. Prior experience with texture analysis using a variety of texture parameters (i.e., co-occurrence matrix, run-length matrix, absolute gradient method, histogram method) failed to establish laterality in cases of unilateral hippocampal sclerosis yet clearly differentiated between a group with hippocampal sclerosis and one with normal hippocampi (Bonilha et al., 2003). In texture analysis studies, MR imaging data are acquired on subjects using a fixed protocol. Texture features are calculated in ROIs that are usually drawn manually. The best set of features is then selected by maximizing the classification accuracy in a set of samples. Combination of more than two features may result in a higher classification rate. However, due to the small sample size (36 mTLE patients), to avoid the problem of curse of dimensionality, we did not use more than two features, as the ratio of the number of samples and the number of features is suggested to be at least 10–20 (Theodoridis and Koutroumbas, 2006). Co-occurrence matrices, thought to be more suited to address the boundary problem, have been more popular in these applications, particularly for small ROIs or ROIs with twisted

shapes (Garcia-Sevilla and Petrou, 2001). However, wavelet analysis has been found to outperform the co-occurrence matrix application because of its ability to analyze images in different resolutions (Henke-Reed and Cheng, 1993; Randen and Husoy, 1999). The issue of the ROI boundary problem, although manageable by the method described (Fig. 4), requires further refinement. A small ROI, as in the case of a reduced hippocampal volume, in the absence of much interhippocampal asymmetry in signal intensity, may also limit applicability of texture analysis.

The employed translation-invariant wavelet decomposition is not rotation-invariant. Rotation invariance in texture analysis is important when the texture is found to be directional (Jafari-Khouzani and Soltanian-Zadeh, 2005). The laminar structure of the hippocampus remains identical from slice-to-slice along its axis. Thus, with a standard head position for imaging, rotational variability should be appreciably lessened. Signal-to-noise ratio (SNR) is usually lower with higher image resolution (i.e., first level of decomposition) as the power of natural signals is lower with higher frequencies. Optimal wavelet features were identified at the second level of decomposition and are thus less affected by noise.

Texture features of MR images are subject to significant variability attributable to MRI design and protocol. In most investigations, the MRI unit and protocols are fixed for a set of experiments. Gray level normalization methods are helpful for establishing uniformity in textural analysis also. For the widespread use of textural analysis, it is necessary to define features that are reproducible and transferable among MR imaging centers. This has proven difficult as identified in a multicenter trial using a fixed protocol on reticulated foam test objects, in which it was concluded that texture measurements were, in fact, not transportable among centers (Lerski et al., 1999).

Image intensity may alter from patient-to-patient because of inevitable tissue variations from one patient to another. Moreover, image intensity may vary in repeated studies of the same region in the same patient using the same imaging protocol and MR imaging unit. Image intensity may depend on acquisition conditions such as room temperature and hygrometry, calibration adjustment, slice location, $B0$ intensity and receiver gain value. The textural features examined must be invariant to these changes. Hence, in the present study, a ratio of measures of the left and right hippocampi established a set of features for each patient. It should be noted that, while investigating ratios will avoid the problem of variation in the intensity and texture characteristics caused by changes in protocol and MRI equipment, our study design does not allow us to comment on how the technique would perform in the presence of clinically very important bilateral disease.

Another issue involves the quality of the MR images themselves. Image distortion due to the inhomogeneity of the magnetic field must be corrected before feature extraction. Likewise, the image must also have adequate resolution and SNR. As mentioned previously, small images and, consequently, small ROIs are not appropriate for texture analysis in most situations. Texture analysis requires high resolution MRI and, therefore, demands increased scan time to avoid reduction of the SNR; yet, the increased time may introduce motion artifact, thus degrading image quality. One possible solution to this problem is to reduce the field-of-view and the number of image slices. In the end, the best set of acquisition parameters may be obtained by allowing a compromise among the different requirements.

A prospective analysis of preoperative cases is necessary to establish a true predictive accuracy for an approach involving FLAIR MR signal analysis, texture analysis and volumetry. In cases where there is strong electroencephalographic evidence of localization-related epilepsy involving either of the temporal lobes but in the absence of visually distinct differences between the hippocampi, the provision of such postprocessing measures may be of significant help in

lateralizing mTLE should a distinct focality exist. Ultimately, a reduced dependency upon invasive measures of electrographic monitoring would benefit such patients.

Acknowledgments

This work was supported in part by NIH grant R01-EB002450. We also would like to thank Dr. Mohammad Reza Siadat and Lucie Bower for helping with image segmentation and data retrieval.

References

Annegers JF, Hauser WA, Coan SP, Rocca WA. A population-based study of seizures after traumatic brain injuries. N Engl J Med 1998;338:20–24. [PubMed: 9414327]

Antel SB, Collins DL, Bernasconi N, Andermann F, Shinghal R, Kearney RE, Arnold DL, Bernasconi A. Automated detection of focal cortical dysplasia lesions using computational models of their MRI characteristics and texture analysis. Neuroimage 2003;19:1748–1759. [PubMed: 12948729]

Babb, TL.; Jann Brown, W. Pathological findings in epilepsy. In: Engel, JJ., editor. Surgical Treatment of the Epilepsies. New York: Raven Press; 1987. p. 511-540.

Bernasconi A, Antel SB, Collins DL, Bernasconi N, Olivier A, Dubeau F, Pike GB, Andermann F, Arnold DL. Texture analysis and morphological processing of magnetic resonance imaging assist detection of focal cortical dysplasia in extra-temporal partial epilepsy. Ann Neurol 2001;49:770–775. [PubMed: 11409429]

Bernasconi A, Bernasconi N, Caramanos Z, Reutens DC, Andermann F, Dubeau F, Tampieri D, Pike BG, Arnold DL. T2 relaxometry can lateralize mesial temporal lobe epilepsy in patients with normal MRI. Neuroimage 2000;12:739–746. [PubMed: 11112405]

Bonilha L, Kobayashi E, Castellano G, Coelho G, Tinois E, Cendes F, Li LM. Texture analysis of hippocampal sclerosis. Epilepsia 2003;44:1546–1550. [PubMed: 14636326]

Briellmann RS, Kalnins RM, Berkovic SF, Jackson GD. Hippocampal pathology in refractory temporal lobe epilepsy: T2-weighted signal change reflects dentate gliosis. Neurology 2002;58:265–271. [PubMed: 11805255]

Carne RP, O'Brien TJ, Kilpatrick CJ, MacGregor LR, Hicks RJ, Murphy MA, Bowden SC, Kaye AH, Cook MJ. MRI-negative PET-positive temporal lobe epilepsy: a distinct surgically remediable syndrome. Brain 2004;127:2276–2285. [PubMed: 15282217]

Cendes F, Leproux F, Melanson D, Ethier R, Evans A, Peters T, Andermann F. MRI of amygdala and hippocampus in temporal lobe epilepsy. J Comput Assist Tomogr 1993;17:206–210. [PubMed: 8454746]

Chupin M, Hammers A, Liu RS, Colliot O, Burdett J, Bardinet E, Duncan JS, Garnero L, Lemieux L. Automatic segmentation of the hippocampus and the amygdala driven by hybrid constraints: method and validation. Neuroimage 2009;46:749–761. [PubMed: 19236922]

Coan AC, Bonilha L, Morgan PS, Cendes F, Li LM. T2-weighted and T2 relaxometry images in patients with medial temporal lobe epilepsy. J Neuroimaging 2006;16:260–265. [PubMed: 16808828]

Criminisi A, Perez P, Toyama K. Region filling and object removal by exemplar-based image inpainting. IEEE Trans Image Process 2004;13:1200–1212. [PubMed: 15449582]

Daubechies, I. Society for Industrial and Applied Mathematics. Philadelphia, pa: 1992. Ten lectures on wavelets.

Didelot A, Ryvlin P, Lothe A, Merlet I, Hammers A, Mauguiere F. PET imaging of brain 5-HT1A receptors in the preoperative evaluation of temporal lobe epilepsy. Brain 2008;131:2751–2764. [PubMed: 18790822]

Duvernoy, HM. The human hippocampus: functional anatomy, vascularization, and serial sections with MRI. 3rd ed.. New York: Springer, Berlin; 2005.

Efros, AA.; Leung, TK. IEEE Comput. Soc. Los Alamitos, CA, USA: 1999. Texture synthesis by non-parametric sampling; p. 1033-1038.

Engel, JJ. Outcome with respect to epileptic seizures. In: Engel, JJ., editor. Surgical Treatment of the Epilepsies. New York: Raven Press; 1987. p. 553-571.

Fernandez G, Effenberger O, Vinz B, Steinlein O, Elger CE, Dohring W, Heinze HJ. Hippocampal malformation as a cause of familial febrile convulsions and subsequent hippocampal sclerosis. Neurology 1998;50:909–917. [PubMed: 9566371]

Freeborough PA, Fox NC. MR image texture analysis applied to the diagnosis and tracking of Alzheimer's disease. IEEE Trans. Med. Imag 1998;17:475–478.

Gambhir SS, Czernin J, Schwimmer J, Silverman DH, Coleman RE, Phelps ME. A tabulated summary of the FDG PET literature. J Nucl Med 2001;42:1S–93S. [PubMed: 11483694]

Garcia-Sevilla P, Petrou M. Analysis of irregularly shaped texture regions. Comput. Vision Image Understand 2001;84:62–76.

Grunewald RA, Jackson GD, Connelly A, Duncan JS. MR detection of hippocampal disease in epilepsy: factors influencing T2 relaxation time. AJNR Am J Neuroradiol 1994;15:1149–1156. [PubMed: 8073986]

Hammers A, Heckemann R, Koepp MJ, Duncan JS, Hajnal JV, Rueckert D, Aljabar P. Automatic detection and quantification of hippocampal atrophy on MRI in temporal lobe epilepsy: a proof-of-principle study. Neuroimage 2007;36:38–47. [PubMed: 17428687]

Heier LA, Bauer CJ, Schwartz L, Zimmerman RD, Morgello S, Deck MD. Large Virchow-Robin spaces: MR-clinical correlation. AJNR Am J Neuroradiol 1989;10:929–936. [PubMed: 2505536]

Henke-Reed MB, Cheng SNC. Cloth texture classification using the wavelet transform. J. Imaging Sci. Technol 1993;37:610–614.

Herlidou-Meme S, Constans JM, Carsin B, Olivie D, Eliat PA, Nadal-Desbarats L, Gondry C, Le Rumeur E, Idy-Peretti I, de Certaines JD. MRI texture analysis on texture test objects, normal brain and intracranial tumors. Magn Reson Imaging 2003;21:989–993. [PubMed: 14684201]

Jack CR Jr. Hippocampal T2 relaxometry in epilepsy: past, present, and future. AJNR Am J Neuroradiol 1996;17:1811–1814. [PubMed: 8933862]

Jack CR Jr. Krecke KN, Luetmer PH, Cascino GD, Sharbrough FW, O'Brien PC, Parisi JE. Diagnosis of mesial temporal sclerosis with conventional versus fast spin-echo MR imaging. Radiology 1994;192:123–127. [PubMed: 8208923]

Jack CR Jr. Rydberg CH, Krecke KN, Trenerry MR, Parisi JE, Rydberg JN, Cascino GD, Riederer SJ. Mesial temporal sclerosis: diagnosis with fluid-attenuated inversion-recovery versus spin-echo MR imaging. Radiology 1996;199:367–373. [PubMed: 8668780]

Jack CR Jr. Sharbrough FW, Twomey CK, Cascino GD, Hirschorn KA, Marsh WR, Zinsmeister AR, Scheithauer B. Temporal lobe seizures: lateralization with MR volume measurements of the hippocampal formation. Radiology 1990;175:423–429. [PubMed: 2183282]

Jackson GD, Connelly A, Duncan JS, Grunewald RA, Gadian DG. Detection of hippocampal pathology in intractable partial epilepsy: increased sensitivity with quantitative magnetic resonance T2 relaxometry. Neurology 1993;43:1793–1799. [PubMed: 8414034]

Jackson GD, Kuzniecky RI, Cascino GD. Hippocampal sclerosis without detectable hippocampal atrophy. Neurology 1994;44:42–46. [PubMed: 8290088]

Jafari-Khouzani, K.; Siadat, MR.; Soltanian-Zadeh, H.; Elisevich, K. Texture analysis of hippocampus for epilepsy; Proc. SPIE Med Imag. SPIE-Int. Soc. Opt. Eng; San Diego, CA, USA: 2003. p. 279-288.

Jafari-Khouzani K, Soltanian-Zadeh H. Radon transform orientation estimation for rotation invariant texture analysis. IEEE Trans Pattern Anal Mach Intell 2005;27:1004–1008. [PubMed: 15945146]

Jenkinson M, Smith S. A global optimisation method for robust affine registration of brain images. Med Image Anal 2001;5:143–156. [PubMed: 11516708]

Kim JH, Tien RD, Felsberg GJ, Osumi AK, Lee N. MR measurements of the hippocampus for lateralization of temporal lobe epilepsy: value of measurements of the body vs the whole structure. AJR Am J Roentgenol 1994;163:1453–1457. [PubMed: 7992746]

Kobayashi E, D'Agostino MD, Lopes-Cendes I, Berkovic SF, Li ML, Andermann E, Andermann F, Cendes F. Hippocampal atrophy and T2-weighted signal changes in familial mesial temporal lobe epilepsy. Neurology 2003;60:405–409. [PubMed: 12578919]

Kodama N, Takeuchi H. Correlation between cerebral atrophy and texture features in Alzheimer-type dementia brains: a 3-year follow-up MRI study. Trans. Inst. Elec. Eng. Japan, Part C 2005;125-C: 1382–1386.

Lehericy S, Dormont D, Semah F, Clemenceau S, Granat O, Marsault C, Baulac M. Developmental abnormalities of the medial temporal lobe in patients with temporal lobe epilepsy. AJNR Am J Neuroradiol 1995;16:617–626. [PubMed: 7611013]

Lerski RA, Schad LR, Luypaert R, Amorison A, Muller RN, Mascaro L, Ring P, Spisni A, Zhu X, Bruno A. Multicentre magnetic resonance texture analysis trial using reticulated foam test objects. Magn Reson Imaging 1999;17:1025–1031. [PubMed: 10463653]

Liu, Y.; Teverovskiy, L.; Carmichael, O.; Kikinis, R.; Shenton, M.; Carter, CS.; Stenger, VA.; Davis, S.; Aizenstein, H.; Becker, JT.; Lopez, OL.; Meltzer, CC. Int Conf Med Image Comput Comput Assist Interv. Saint-Malo, France: Springer-Verlag; 2004. Discriminative MR image feature analysis for automatic schizophrenia and Alzheimer's disease classification; p. 393-401.

Maclullich AM, Wardlaw JM, Ferguson KJ, Starr JM, Seckl JR, Deary IJ. Enlarged perivascular spaces are associated with cognitive function in healthy elderly men. J Neurol Neurosurg Psychiatry 2004;75:1519–1523. [PubMed: 15489380]

Mallat, SG. A wavelet tour of signal processing. 2nd ed.. San Diego: Academic Press; 1999.

Melhem ER, Whitehead RE, Bert RJ, Caruthers SD. MR imaging of the hippocampus: measurement of T2 with four dual-echo techniques. Radiology 1998;209:551–555. [PubMed: 9807588]

Merlet I, Ostrowsky K, Costes N, Ryvlin P, Isnard J, Faillenot I, Lavenne F, Dufournel D, Le Bars D, Mauguiere F. 5-HT1A receptor binding and intracerebral activity in temporal lobe epilepsy: an [18F] MPPF-PET study. Brain 2004;127:900–913. [PubMed: 14985263]

Mojsilovic A, Popovic MV, Rackov DM. On the selection of an optimal wavelet basis for texture characterization. IEEE Trans Image Process 2000;9:2043–2050. [PubMed: 18262942]

O'Brien TJ, David EP, Kilpatrick CJ, Desmond P, Tress B. Contrast-enhanced perfusion and diffusion MRI accurately lateralize temporal lobe epilepsy: a pilot study. J Clin Neurosci 2007;14:841–849. [PubMed: 17596947]

Okujava M, Schulz R, Ebner A, Woermann FG. Measurement of temporal lobe T2 relaxation times using a routine diagnostic MR imaging protocol in epilepsy. Epilepsy Res 2002;48:131–142. [PubMed: 11823117]

Pesquet JC, Krim H, Carfantan H. Time-invariant orthonormal wavelet representations. IEEE Transactions on Signal Processing 1996;44:1964–1970.

Randen T, Husoy JH. Filtering for texture classification: a comparative study. IEEE Trans. Pattern Anal. Mach. Intell 1999;21:291–310.

Rodionov R, Chupin M, Williams E, Hammers A, Kesavadas C, Lemieux L. Evaluation of atlas-based segmentation of hippocampi in healthy humans. Magn Reson Imaging. 2009

Shorvon, SD. Magnetic resonance scanning and epilepsy. New York: Plenum Press; 1994.

Smith SM. Fast robust automated brain extraction. Hum Brain Mapp 2002;17:143–155. [PubMed: 12391568]

Tan KM, Britton JW, Buchhalter JR, Worrell GA, Lagerlund TD, Shin C, Cascino GD, Meyer FB, So EL. Influence of subtraction ictal SPECT on surgical management in focal epilepsy of indeterminate localization: a prospective study. Epilepsy Res 2008;82:190–193. [PubMed: 18835758]

Theodoridis, S.; Koutroumbas, K. Pattern recognition. 3rd ed.. San Diego: Academic Press; 2006.

Toczek MT, Carson RE, Lang L, Ma Y, Spanaki MV, Der MG, Fazilat S, Kopylev L, Herscovitch P, Eckelman WC, Theodore WH. PET imaging of 5-HT1A receptor binding in patients with temporal lobe epilepsy. Neurology 2003;60:749–756. [PubMed: 12629228]

Van Paesschen W. Quantitative MRI of Mesial Temporal Structures in Temporal Lobe Epilepsy 1997:3–12.

Van Paesschen W, Sisodiya S, Connelly A, Duncan JS, Free SL, Raymond AA, Grunewald RA, Revesz T, Shorvon SD, Fish DR, et al. Quantitative hippocampal MRI and intractable temporal lobe epilepsy. Neurology 1995;45:2233–2240. [PubMed: 8848199]

Wehner T, Lapresto E, Tkach J, Liu P, Bingaman W, Prayson RA, Ruggieri P, Diehl B. The value of interictal diffusion-weighted imaging in lateralizing temporal lobe epilepsy. Neurology 2007;68:122–127. [PubMed: 17210892]

Woermann FG, Barker GJ, Birnie KD, Meencke HJ, Duncan JS. Regional changes in hippocampal T2 relaxation and volume: a quantitative magnetic resonance imaging study of hippocampal sclerosis. J Neurol Neurosurg Psychiatry 1998;65:656–664. [PubMed: 9810933]

Yu O, Mauss Y, Namer IJ, Chambron J. Existence of contralateral abnormalities revealed by texture analysis in unilateral intractable hippocampal epilepsy. Magn Reson Imaging 2001;19:1305–1310. [PubMed: 11804758]

Yu O, Mauss Y, Zollner G, Namer IJ, Chambron J. Distinct patterns of active and non-active plaques using texture analysis on brain NMR images in multiple sclerosis patients: preliminary results. Magn Reson Imaging 1999;17:1261–1267. [PubMed: 10576711]

Yu O, Roch C, Namer IJ, Chambron J, Mauss Y. Detection of late epilepsy by the texture analysis of MR brain images in the lithium-pilocarpine rat model. Magn Reson Imaging 2002;20:771–775. [PubMed: 12591572]

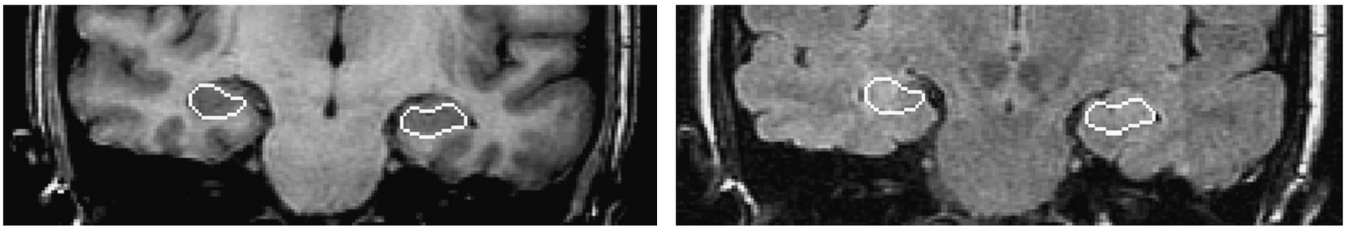

Fig. 1.
Manual segmentation of the hippocampi in a representative coronal T1-weighted MR image and its map on the FLAIR MRI.

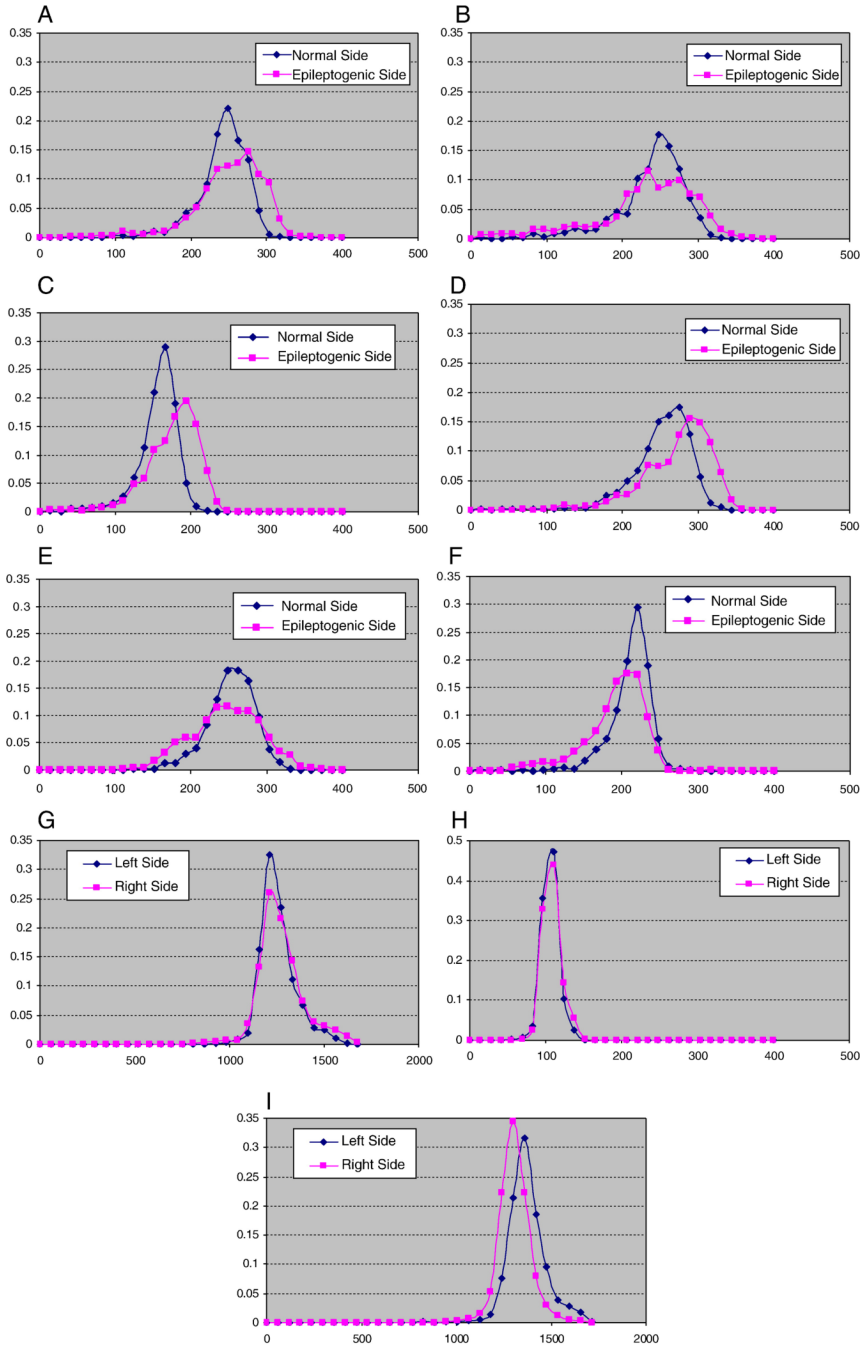

Fig. 2.

Normalized histogram (i.e., number of voxels for each intensity level divided by the total number of voxels in the hippocampus) of hippocampal FLAIR signal intensities in six selected cases of mTLE patients as well as three normal controls. Normalization is required in order to compare adequately the histograms of each side as the volumes of the two sides may differ and thus affect the number of voxels for each intensity level. A: case 4; B: case 10. Examples of patients requiring extraoperative ECoG. C: case 27; D: case 34; E: case 31; and F: case 29. Examples of patients who proceeded to surgery without intracranial study. In each of these six cases, the epileptogenic side is characterized by a greater variance of intensity but not in all cases is there a greater mean signal intensity (B, E, F). (G and H) Histograms of control subjects

show that both mean signal intensity and variance are nearly identical. (I) Histogram of a control subject in whom the mean signals appear different but the variance again is nearly identical.

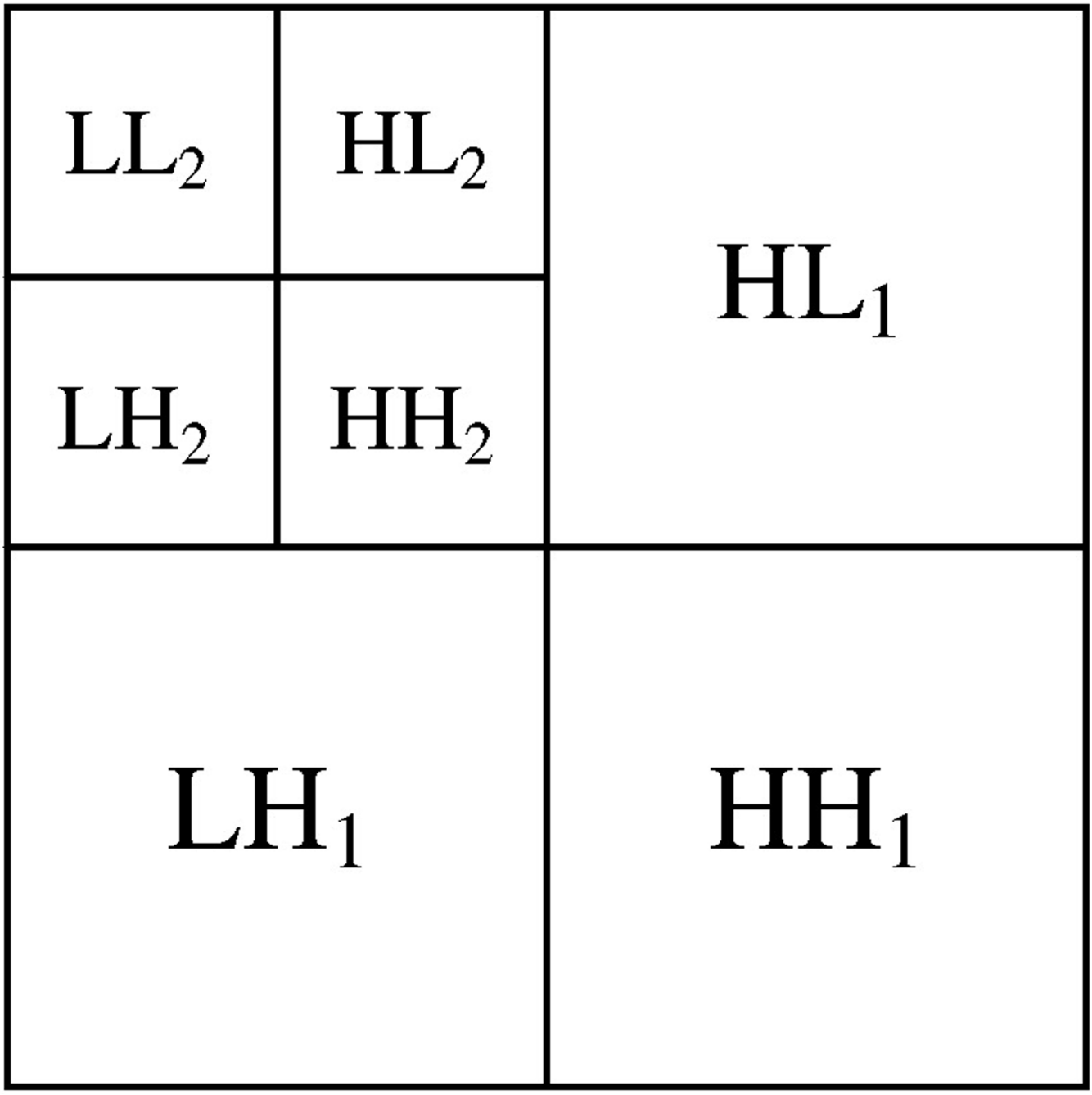

Fig. 3.
Subbands produced by two levels of ordinary wavelet decomposition.

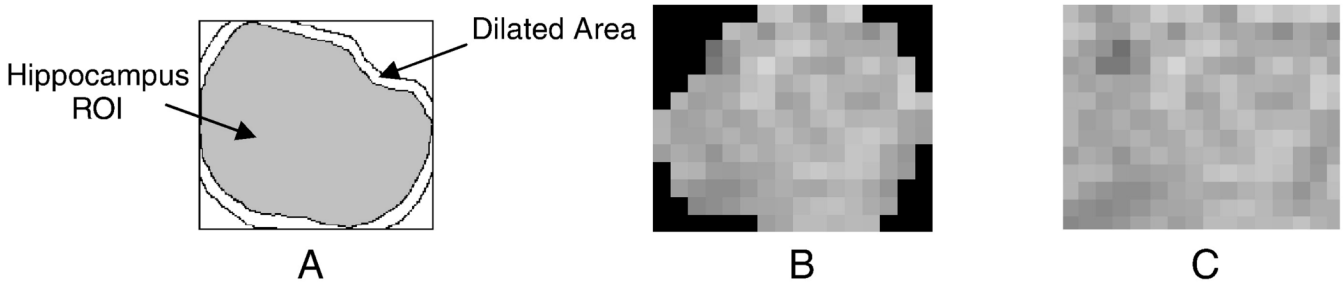

Fig. 4.
(A) Filling out the empty area by repetitive dilations of the hippocampus ROI and exemplar-based texture inpainting. (B) ROI before processing. (C) ROI after processing.

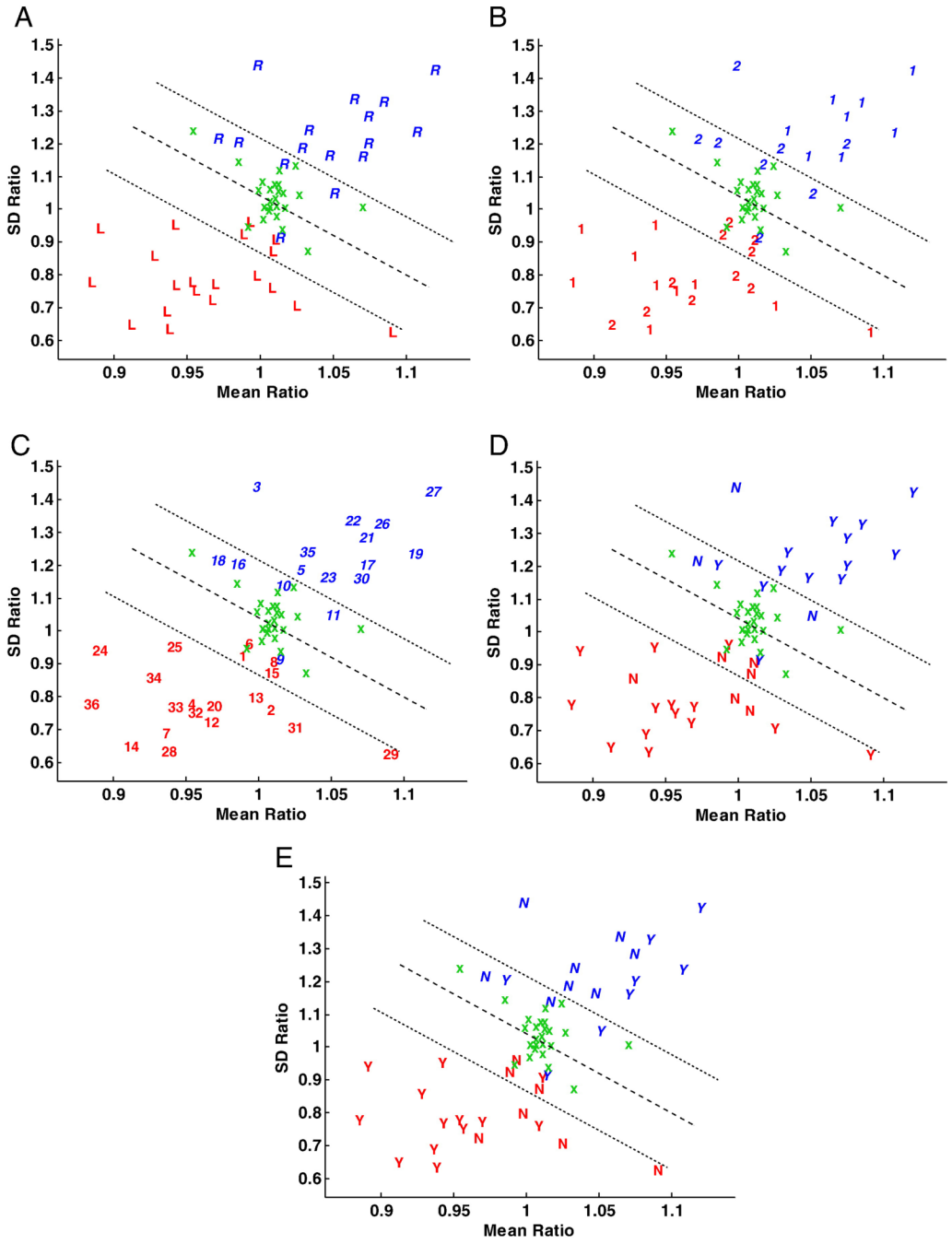

Fig. 5.

Scatter plots of the mean and standard deviation ratios (right/left) of FLAIR MR signal intensity. (A) Cases are distinguished by the symbols, 'R' and 'L', respectively, corresponding to individual cases in which the right or left hippocampus was judged to be epileptogenic according to Engel Class Ia outcome. The symbol 'x' represents control subjects. The linear classifier shows there to be a good separation of sides of epileptogenicity. (B) Cases are distinguished according to whether they required solely scalp electroencephalographic application to distinguish laterality ('1') or further extraoperative ECoG ('2'). (C) Cases are identified by their numerical assignment for cross-referencing of clinical profiles (see Table 1). (D) Cases are distinguished by the symbols, 'Y' and 'N', respectively, according to whether

medial temporal sclerosis (MTS) was appreciated by qualitative assessment of MR images with those identified as MTS labeled ‘Y’ and the others, ‘N’. (E) Cases identified with Ammon's horn sclerosis after pathological review are identified by the symbol ‘Y’ and those without, ‘N’.

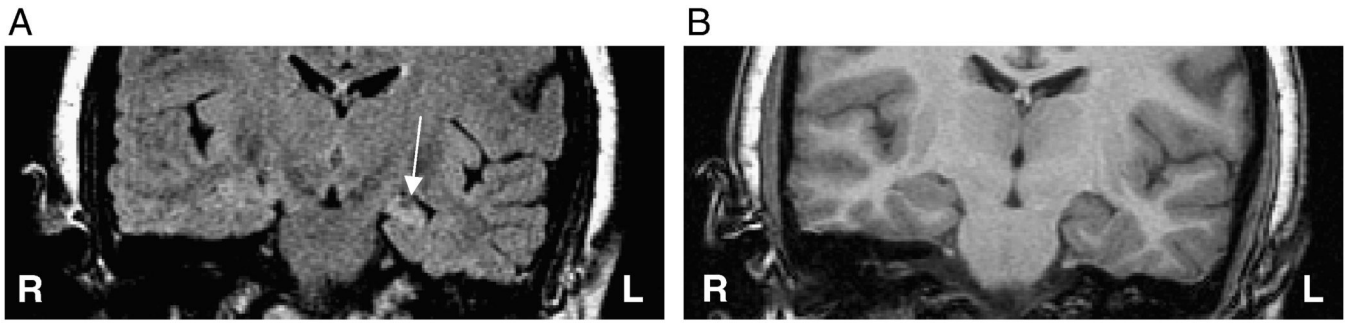

Fig. 6.
Case 4: FLAIR (A) and T1-weighted (B) MR coronal images of a correctly lateralized left mTLE as established by mean and standard deviation ratios of FLAIR MR signal intensities in a case requiring extraoperative ECoG.

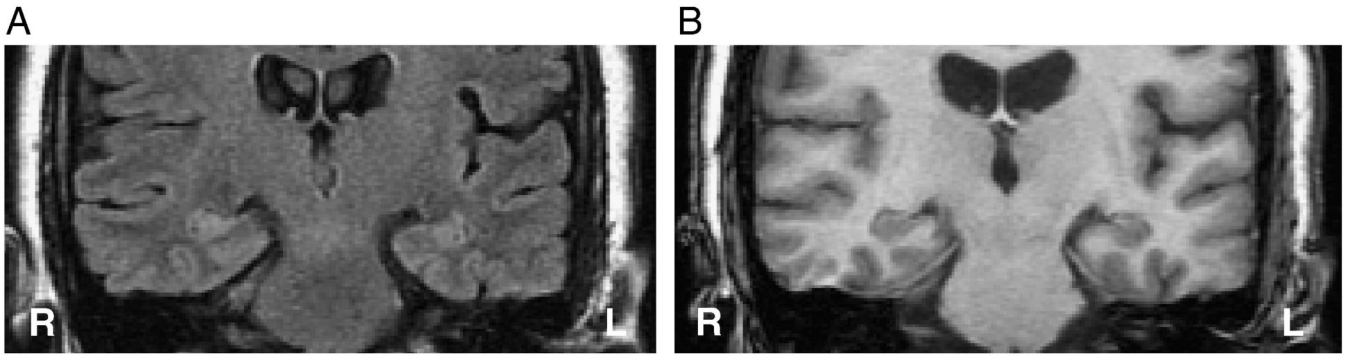

Fig. 7.

Case 11: FLAIR (A) and T1-weighted (B) MR coronal images in a case of right mTLE in which both hippocampi appear similar by visual inspection and for which extraoperative ECoG was required. The mTLE was correctly lateralized using the mean and standard deviation ratios of FLAIR MR signal intensities. This case was plotted inside the boundary domain in the latter feature set (see Fig. 5C).

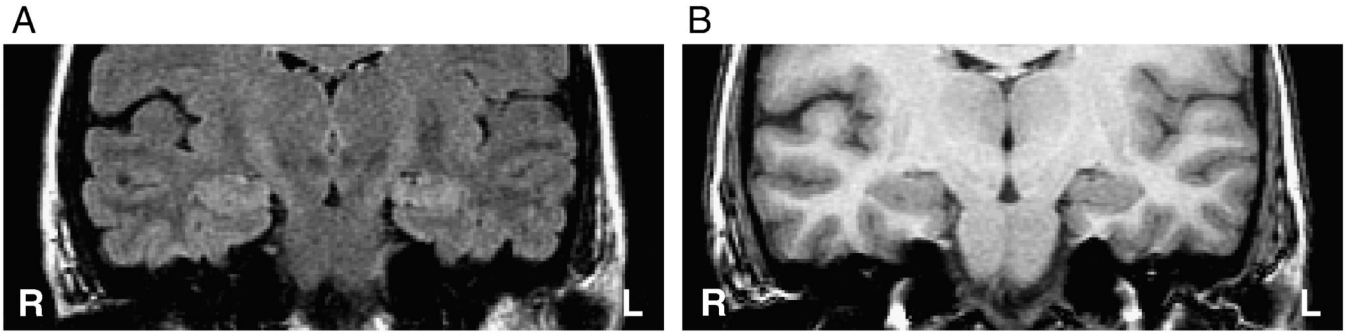

Fig. 8.

Case 15: FLAIR (A) and T1-weighted (B) MR coronal images in a case of left mTLE in which both hippocampi appear similar by visual inspection and for which extraoperative ECoG was required. The laterality of the mTLE was misclassified by volumetric analysis but correctly classified using the mean and standard deviation ratios of FLAIR MR signal intensities. This case was plotted inside the boundary domain in the latter feature set (see Fig. 5C).

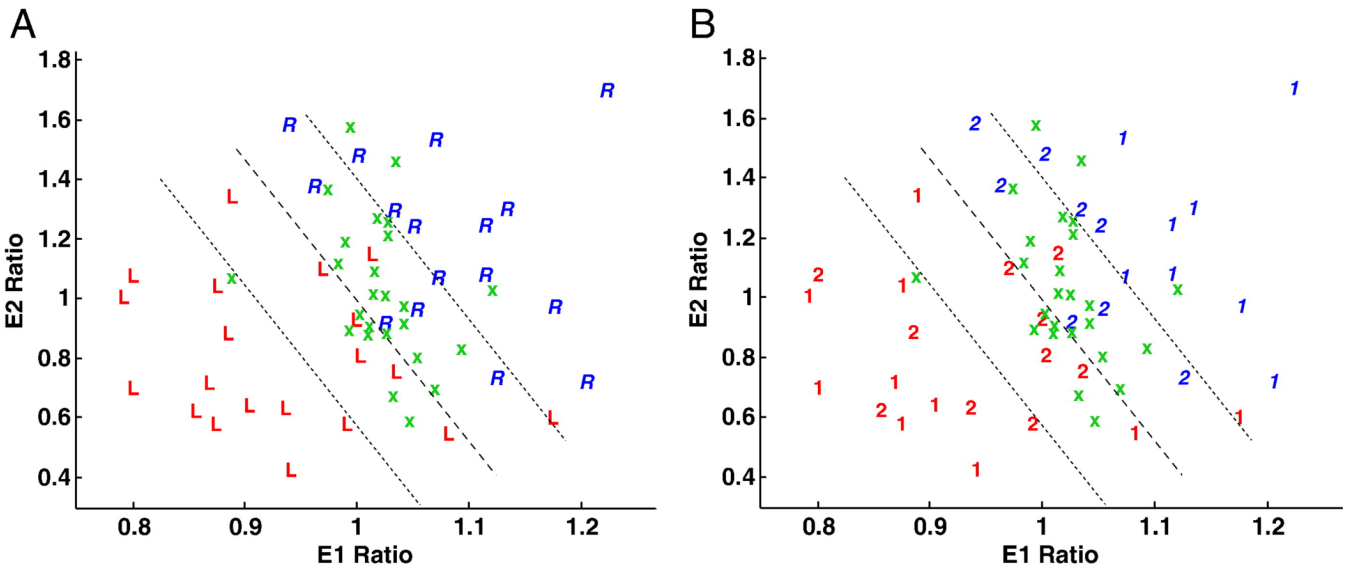

Fig. 9.

Scatter plot of two selected wavelet energy features corresponding to the two low-resolution subbands (E_1 and E_2) with wavelet basis db8 and expressed as ratios (right/left) (see Fig. 5). (A) The symbols, 'R' and 'L', respectively, correspond to the patients with right and left abnormal (epileptogenic) hippocampi. These are separated by a linear discriminator line traversing a central cluster depicting the results for control subjects ('x'). Certain cases under study are identified in this central cluster and therefore cannot be adequately separated from control subjects despite correct segregation by the discriminator line itself. (B) Cases are distinguished according to their requirement for extraoperative ECoG (i.e., '1' indicating those cases proceeding to surgery without such study and '2', those cases requiring it).

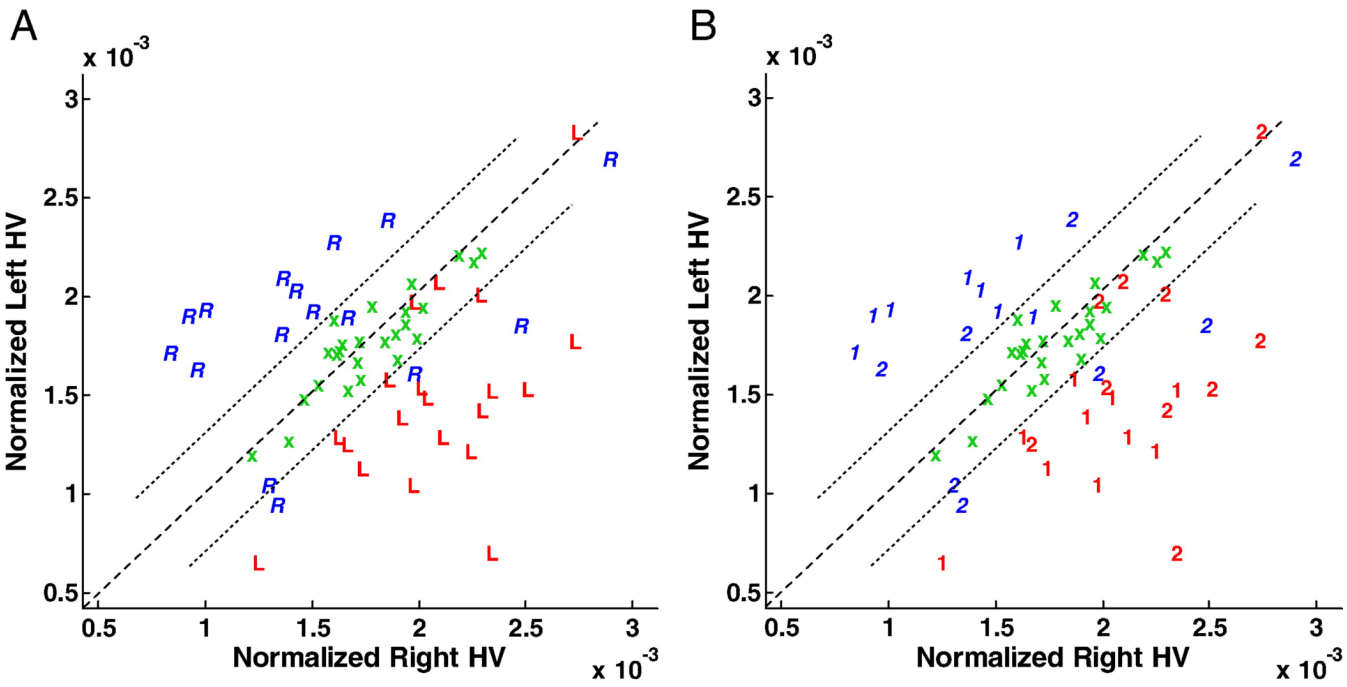

Fig. 10.

Linear scatter plot of normalized hippocampal volumes (HVs) showing the distribution of control subjects ('x') and study cases according to their laterality for epileptogenicity (i.e., right vs. left) and their requirement for intracranial electrographic study. The volumes of control subjects are clustered and define the linear boundary (i.e., control) domain within which the separation of a right- or left-sided mTLE may not be possible. (A) All patients are represented as a right- or left-sided mTLE of which 5 cases (2 R, 3 L) fall within the control domain. (B) Patients proceeding to resection without the need for extraoperative ECoG ('1') and those who required intracranial study prior to resection ('2') are identified. Note that only 1 case of the former group fall within the control domain.

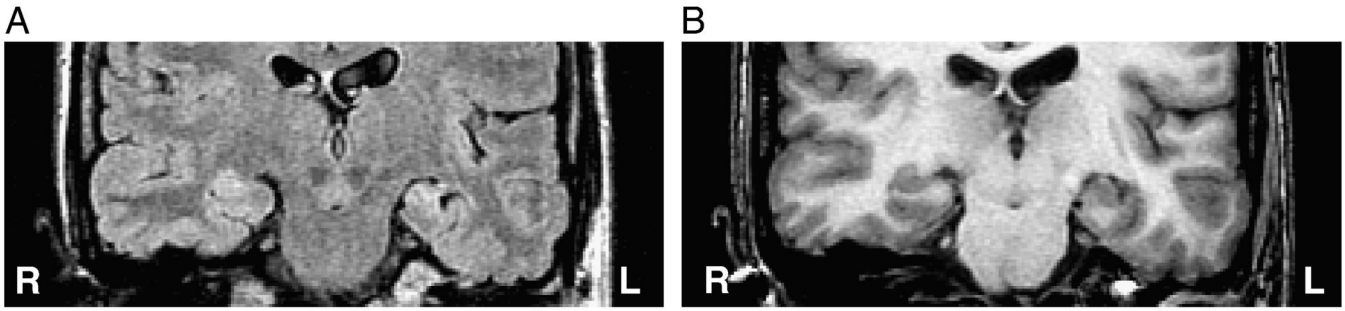

Fig. 11.

Case 9: FLAIR (A) and T1-weighted (B) MR coronal images in a case of right mTLE which was misclassified by two feature sets. This case was plotted inside the boundary domain of the graph of the mean and standard deviation ratios of FLAIR MR signal intensities (see Fig. 5C). The images demonstrate an asymmetry across the midline as noted by an inequality of ventricular outline, the crus of the fornix, brainstem contour and the relative vertical displacement of the Sylvian fissures.

Neuroimage. Author manuscript; available in PMC 2011 January 15.

Table 1

Clinical profiles and hippocampal volumes of study patients. Patients are identified by gender, the need for intracranial electrographic study (II) in addition to the preliminary scalp EEG study (I), side of surgery, age at surgery, duration of epilepsy, and duration of followup. The likely initial precipitating event (risk) causing the epilepsy is provided along with the age at which it occurred, if known. The presence or absence of mesial temporal sclerosis (MTS) according to the radiologist's report establishes the preoperative qualitative interpretation. Histopathology, when available, indicates the main feature of the interpretation. The volumes of both left and right hippocampi and the relative difference (left – right) between the two indicate that a negative outcome implicates but does not necessarily confirm a left mTLE when comparison is made with the side of surgery. Normalization ((L – R)/R) allows a comparison among cases. The control subjects had an average hippocampal volume of 2507 mm^3 on the left side and 2510 mm^3 on the right side. Abbreviations: I, inpatient scalp EEG study; II, extraoperative ECoG; AHS, Ammon's horn sclerosis; CA, corpora amylacea; CHI, closed head injury; F, female; FH, family history; FS, febrile seizure; Hipp, hippocampal; L, left; M, male; MDG, microdysgenesis; NF1, neurofibromatosis type 1; N, no; PNI, perinatal ischemia; R, right; Vol, volume; Y, yes; y, year.

Patient Number	Gender	EEG	Side	Age at Surgery	Duration of Epilepsy (y)	Duration of followup (y)	Risk	MTS	Pathology	Left Hipp Vol (mm^3)	Right Hipp Vol (mm^3)	Relative Difference (L-R)/R
1	F	I/II	L	30	23	9	CHI(2y);FH	N	gliosis	3026.6	3047.4	−0.01
2	F	I/II	L	26	25	9	meningitis	N	AHS	1512.7	2486.2	−0.39
3	F	I/II	R	34	32	6	FS(2y);FH	N	-	2625.3	1961.6	0.34
4	F	I/II	L	50	49	10	FS(1y);FH	Y	AHS	1645.7	2193.4	−0.25
5	F	I/II	R	31	19	6	CHI(4,11y)	Y	MDG	2808.3	3757.4	−0.25
6	M	I/II	L	31	26	7	FH	Y	-	2297.1	2622.8	−0.12
7	F	I/II	L	65	15	9	encephalitis	Y	AHS	904.0	3016.9	−0.70
8	F	I/II	L	54	40	6	NF1	N	AHS	2289.8	3543.9	−0.35
9	F	I/II	R	40	19	10	CHI(17,21y)	Y	AHS	1339.5	1882.3	−0.29
10	M	I/II	R	52	50	7	-	Y	CA	2349.6	1381.0	0.70
11	F	I/II	R	66	16	10	meningioma	N	AHS	2655.8	2853.4	−0.07
12	F	I/II	L	37	20	7	-	Y	gliosis	1603.0	2587.5	−0.38
13	F	I/II	L	43	15	8	CHI	N	MDG	2600.9	2630.2	−0.01
14	M	I/II	L	32	28	9	kernicterus	Y	AHS	2230.0	2921.7	−0.24
15	F	I/II	L	54	40	11	encephalitis	N	gliosis	2909.5	2822.9	0.03
16	M	I/II	R	53	46	2	meningitis	Y	AHS	1492.1	1842.5	−0.19
17	F	I/II	R	15	11	2	FS;FH	Y	AHS	3084.9	2386.8	0.29
18	F	I/II	R	31	15	3	CHI;FH	N	-	2428.7	2978.7	−0.18
19	F	I	R	37	30	9	prematurity	Y	AHS	2827.8	1988.5	0.42

Patient Number	Gender	EEG	Side	Age at Surgery	Duration of Epilepsy (y)	Duration of followup (y)	Risk	MTS	Pathology	Left Hipp Vol (mm^3)	Right Hipp Vol (mm^3)	Relative Difference (L-R)/R
20	M	I	L	53	16	7	CHI;FH	Y	AHS	2452.0	3379.2	−0.27
21	M	I	R	36	33	9	meningitis	Y	gliosis	2477.7	1196.7	1.07
22	F	I	R	38	26	9	FS;FH	Y	gliosis	2526.5	1307.8	0.93
23	F	I	R	34	24	9	FS;CHI	Y	CA	2755.8	1333.4	1.07
24	M	I	L	47	48	9	-	Y	AHS	1751.8	2697.2	−0.35
25	M	I	L	40	32	7	-	Y	AHS	1914.1	2419.1	−0.21
26	F	I	R	32	20	8	FS	Y	AHS	2266.6	1762.8	0.29
27	M	I	R	26	21	6	PNI	Y	AHS	2940.0	2053.1	0.43
28	F	I	L	56	42	9	-	Y	AHS	1879.9	2902.2	−0.35
29	F	I	L	28	4	8	aneurysm	Y	gliosis	1629.8	3016.9	−0.46
30	F	I	R	45	34	8	FS	Y	AHS	2443.5	2142.2	0.14
31	M	I	L	24	21	9	prematurity	Y	-	2232.5	2639.9	−0.15
32	F	I	L	48	44	7	-	Y	AHS	830.8	1593.2	−0.48
33	M	I	L	20	17	7	CHI	Y	AHS	1777.4	3368.2	−0.47
34	F	I	L	48	22	9	CHI	N	AHS	1540.8	2537.4	−0.39
35	F	I	R	50	23	8	CHI	Y	-	2859.5	1859.2	0.54
36	F	I	L	52	31	2	CHI; fever	Y	AHS	1926.8	2676.4	−0.28

Table 2

Comparative classification accuracies using the introduced feature sets reported and the employed number of features.

#	Feature Set	Number of Features	Range for patients	Accuracy (percentage) respectively with and, in brackets, without considering the boundary domain
1	Mean value	1	1.00±0.1	58 (86)
2	Standard deviation	1	0.98±0.5	72 (98)
3	Mean and standard deviation	2	-	75 (**98**)
4	Wavelet signatures using db4	2 (E_1, E_2)	-	64 (92)
5	Wavelet signatures using db6	2 (E_1, E_2)	-	64 (92)
6	Wavelet signatures using db8	2 (E_1, E_2)	-	64 (**94**)
7	Volume (right/left)	1	1.2±1.1	75 (83)

Table 3

Misclassified and within-boundary domain cases assessed by different feature sets reported with their lateralization as determined by Engel class Ia outcome.

Feature Set	Misclassified (according to the discriminator line)		Inside Linear Boundary Domain	
	Left Sided	Right Sided	Left Sided	Right Sided
Mean and standard deviation	-	9	1,6,8,15	9,10,11,16,18
Wavelet signatures using db8	8, 29	-	1,2,6,8,15,25,31	3,9,11,17,18
Volume	15	5,9,11,16,18	1,13,15	16,30